Journal of Luminescence 157 (2015) 285–292

Contents lists available at ScienceDirect

Journal of Luminescence

journal homepage: www.elsevier.com/locate/jlumin

Luminescence properties of Yb:Nd:Tm:KY_3F_{10} nanophosphor and thermal treatment effects

Laércio Gomes [a,*], Horácio Marconi da Silva M.D. Linhares [a], Rodrigo Uchida Ichikawa [b], Luis Gallego Martinez [b], Izilda Marcia Ranieri [a]

[a] Centro de Lasers e Aplicações, Instituto de Pesquisas Energéticas e Nucleares, IPEN-CNEN/SP, Butantã, P.O. Box 11049, São Paulo, SP o5422-970, Brazil
[b] Departamento de Ciências dos Materiais, Instituto de Pesquisas Energéticas e Nucleares, Brazil

ARTICLE INFO

Article history:
Received 30 April 2014
Received in revised form
22 August 2014
Accepted 25 August 2014
Available online 6 September 2014

Keywords:
Time-resolved luminescence spectroscopy
Rare-earth luminescence
Energy transfer rate parameters
Upconversion luminescence
Luminescence efficiency
Nanophosphors

ABSTRACT

In this work, we present the spectroscopic properties of KY_3F_{10} (KY3F) nanocrystals activated with thulium and codoped with ytterbium and neodymium ions. The most important processes that lead to the thulium upconversion emissions in the blue region were identified. A time-resolved luminescence spectroscopy technique was employed to measure the luminescence decays and to determine the most important mechanisms involved in the upconversion process that populates $^1G_4$ (Tm^{3+}) excited states. Analysis of the energy-transfer processes dynamics using selective pulsed-laser excitations in Yb:Nd:Tm, Nd:KY3F nanocrystals shows that the direct energy transfer from Nd^{3+} to Tm^{3+} ions is the mechanism responsible for the 78% of the blue upconversion luminescence in the Yb:Nd:Tm:KY3F when compared with the Yb:Nd:Tm:KY3F bulk crystal for an laser excitation at 802 nm. An investigation of the $^1G_4$ level luminescence kinetic of Tm^{3+} in Yb/Nd/Tm system revealed that the luminescence efficiency ($^1G_4$) starts with a very low value (0.38%) for the synthesized nanocrystal (as grown) and strongly increases to 97% after thermal treatment at 550 °C for 6 h under argon flow. As a consequence of the thermal treatment at $T=550$ °C, the contributions of the (Nd × Tm) (Up_1) and (Nd × Yb × Tm) (Up_2) upconversion processes to the $^1G_4$ luminescence are 33% (Up_1) and 67% for Up_2. Up_2 process represented by Nd^{3+} ($^4F_{3/2}$)→Yb^{3+} ($^2F_{7/2}$) followed by Yb^{3+} ($^2F_{5/2}$)→Tm ($^3H_4$)→Tm^{3+} ($^1G_4$) was previously reported as the main mechanism to produce the blue luminescence in Yb:Nd:Tm:$YLiF_4$ and KY_3F_{10} bulk crystals. Results of X-ray diffraction analysis of nanopowder using the Rietveld method reveled that crystallite sizes remain unchanged (12–14 nm) after thermal treatments with $T \leq 400$ °C, while the $^1G_4$ luminescence efficiency strongly increases from 0.38% ($T=25$ °C) to 12% ($T=400$ °C). Results shown that the Nd^{3+} ions distribution has a concentration gradient increasing towards the nanoparticle surface allowing the direct (Nd × Tm) (Up_1) (78%) in competition with the (Nd × Yb × Tm) (Up_2) (22%) upconversions for the synthesized nanocrystals (11 nm).

1. Introduction

With the oncoming of the nanoscience and nanotechnology in the past few decades, this new field has exerted great impact on upconversion materials, then studies on the synthesis and properties of upconversion nanophosphors [1] have received intense research interest due to their application as luminescent labels in bioimaging, and as donors in energy transfer systems [2,3]. Within this aim, fluoride crystals doped with trivalent rare earth ions has extensively studied due to generation of efficient multicolor emission lines in the visible when excited by infrared diode laser near 800 and 970 nm (the optical window for biological samples from 700 to 1200 nm). In particular, KY_3F_{10} (KY3F) crystal has been studied as luminescent materials when activated by several RE^{3+} ions, which can easily substitute Y^{3+} ions in a non-center-symmetrical site [C_{4v} symmetry] [4,5–8]. KY3F is the only compound in the KF–YF_3 system that melts congruently without any phase transition. It crystallizes in the cubic fluorite-type structure (Fm3m) with a lattice parameter $a=11.553$ Å [8], which constitutes an isotropic crystal. In particular, Yb:Nd:Tm:KY_3F_{10} can be synthesized as nanocrystals able to efficiently emit at 482 nm when excited at 802 nm due to its relatively low phonon energy (cut off ~500 cm^{-1}) that is an important point in avoiding energy loss by non-radiative relaxation involving the $^1G_4$ and $^3H_4$ excited levels of Tm^{3+} [9,10].

In this paper, nanocrystals of Yb:Nd:Tm:KY3F sizing 11 nm were synthesized by co-precipitation method in aqueous solution. The multiple processes of energy transfer that occur when this material

* Corresponding author. Tel.: +55 11 31339380.
E-mail address: lgomes@ipen.br (L. Gomes).

http://dx.doi.org/10.1016/j.jlumin.2014.08.048
0022-2313/

is excited around 800 nm were inspected and the transfer rates constants were determined. The upconversion luminescence transient at 482 nm of $^1G_4$ excited state of Tm^{3+} was measured for Yb (10 mol%): Nd(1.3 mol%):Tm(0.5 mol%):KY3F nanocrystals induced by pulsed laser excitation at 802 nm. The luminescence efficiency of $^1G_4$ excited state was determined and its dependence on the thermal treatment temperature and crystallite size were determined.

2. Experimental procedure

The nanopowders were obtained by the coprecipitation method [11,12,13], boiling aqueous solution of potassium fluoride (KF – Merck, 99%) was slowly added in a hot $RECl_3$ aqueous solution (RE=Y, Yb, Nd and Tm), followed by slow addition of an ammonium bifluoride boiling aqueous solution (NH_4HF_2 – Aldrich, 98%). Rare earth fluorides were obtained from ReO_3 (Aldrich, 99.9%) dissolved in concentrated hydrochloric acid. After the addition of the NH_4HF_2 solution a white precipitate was formed, and the resulted solution was maintained at 80 °C and stirring for 3 h. The initial molar proportion was of 1 $KF+(1-x)$ YCl_3+x $LnCl_3+3$ NH_4HF_2, where Ln=Yb, Nd, and Tm. The nanocrystals were separated by centrifugation ($G_{max}=3800$) and the fine powder was collected, washed with Milli-Q water several times and dried in air in a hot plate at 40 °C for 48 h. Thermal treatments at different temperatures were carried out at a resistive oven for 6 h under argon flow (White Martins, 99.995%), using an amount of the synthesized nanopowder and extracting aliquots of it at every interest temperature, to perform the spectroscopic studies.

Samples were characterized by X-ray diffraction (XRD) on a Panalytical X´PERT diffractometer and by transmission electronic microscopy (TEM) on a JEOL JEM 200C microscope with accelerating voltage of 200 kV. Lattice parameters were obtained by Rietveld refinement method using a GSAS-EXPGUI program [14,15] and the mean crystallite diameters (MCD) using Rietveld or the single line methods [16].

The following nanocrystals were synthesized for the luminescence measurements performed in this work: *i*) Yb(10 mol%):Nd (1.3 mol%):Tm(0.5 mol%):KY3F, and *ii*) Nd(1.3 mol%):KY3F.

The absorption spectra of all samples were measured in the range 400–1200 nm at room temperature using a Varian Cary 5000 spectrophotometer working in the diffuse reflection mode. In the luminescence lifetime measurements, the samples were excited by pulsed laser radiation generated by a tunable OPO-IR pumped (Rainbow from OPOTEK, USA) by the second harmonic of a Q-switched Nd:YAG (yttrium aluminum garnet) laser (Brilliant B from Quantel, France). Laser pulse widths of 4 ns at 802 nm were used to directly excite the $^4F_{3/2}$ and $^3H_4$ excited states of Nd^{3+} and Tm^{3+}, respectively. Luminescence signals were analyzed by the 0.25 m Kratos monochromator, detected by the EMI S-20 (or S-1) PMT (response time of 10 ns) or InSb 77 K infrared detector from Judson (response time ~0.5 μs) or using a charge coupled device (CCD) spectrometer coupled to the sample holder containing the nanopowder via optical fiber. Luminescence lifetime was measured using a digital oscilloscope of 100 MS s^{-1} model TDS 410 from TEKTRONIX interfaced to a microcomputer.

3. Experimental results

The synthesized nanopowders have shown the cubic phase ($Fm\bar{3}m$) of KY_3F_{10} corresponding to the fluorite crystalline structure, however with the diffraction peaks wider due to the crystalline planes distortions and defects as seen in Figs. 1 and 2. Nevertheless, X-ray diffraction peaks become narrow after thermal treatment at $T=550$ °C due to the particles growth and increasing of

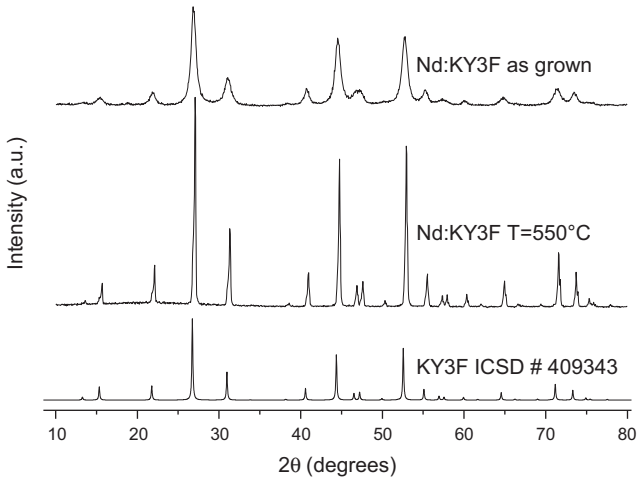

Fig. 1. X-ray diffraction pattern for Nd:KY3F synthesized nanopowder before (as grown) and after thermal treatment ($T=550$ °C). Lowest diffratogram was obtained for a bulk crystal (KY3F) for comparison.

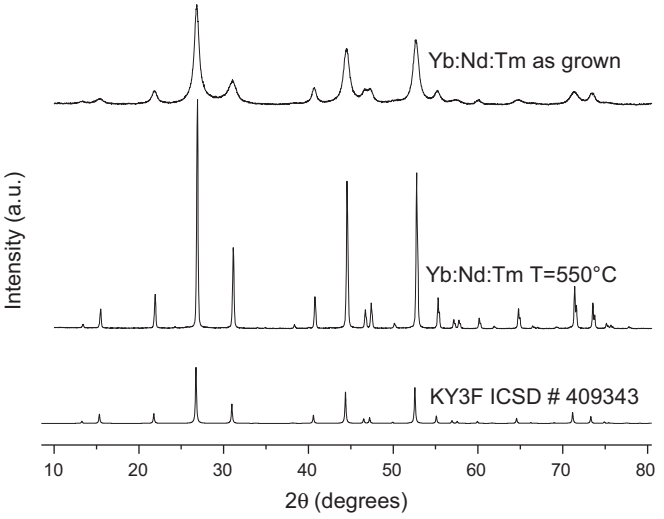

Fig. 2. X-ray diffraction pattern of Yb:Nd:Tm:KY3F synthesized nanopowder before (as grown) and after thermal treatment ($T=550$ °C). Lowest diffratogram was obtained for a bulk crystal (KY3F) for comparison.

crystallinity (Figs. 1 and 2). The synthesized nanocrystals were approximately spherical with a mean diameter of 11 nm as shown by TEM photograph (Fig. 3). After thermal treatment at $T=550$ °C the crystallite grows exhibiting a mean diameter of 198 nm as shown by TEM photograph (Fig. 4) for Nd:KY3F.

Rietveld refinement of the XRD patterns considering the cubic structure with space group $Fm\bar{3}m$ (ICSD 409643) and spherical particles yielded lattice parameters of 11.560 (1) Å and 11.499 (1) Å, and mean crystal size of 11 and 12 nm for the synthesized Nd:KY3F and Yb:Nd:Tm:KY3F nanocrystals, respectively. The smaller cell parameter for the tri-doped sample is due to the codoping with Yb and Tm ions, which have smaller ionic radii than the yttrium one. TEM analysis confirmed the results obtained for the particles sizes. After thermal treatments, the XRD peaks were narrowed due to particles growth and the increasing of crystallinity (Figs. 1 and 2). The changes in the mean crystallite sizes (d) after heating of the samples at diverse temperatures are given in the following:

i) Nd:KY3F
$d=12$ nm (as grown −25 °C); $d=12$ nm ($T=150$ °C); $d=11$ nm

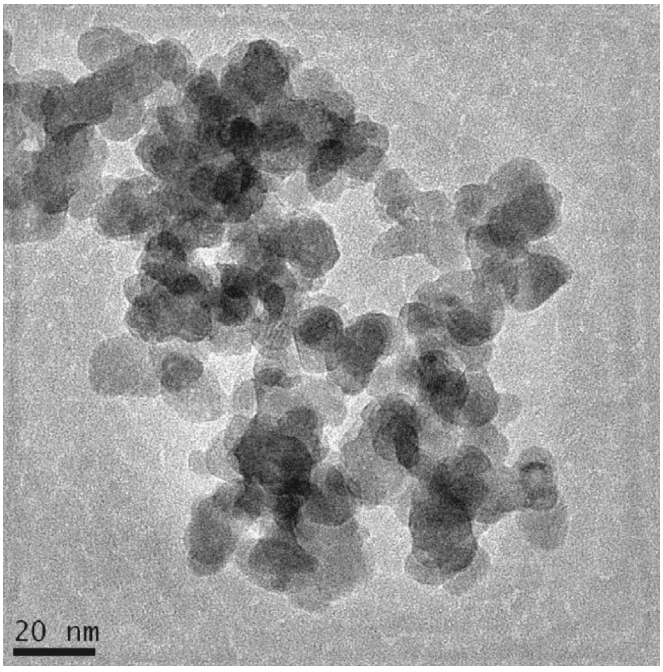

Fig. 3. TEM photograph obtained for Nd:KY3F synthesized nanopowder (as grown) (T=25 °C).

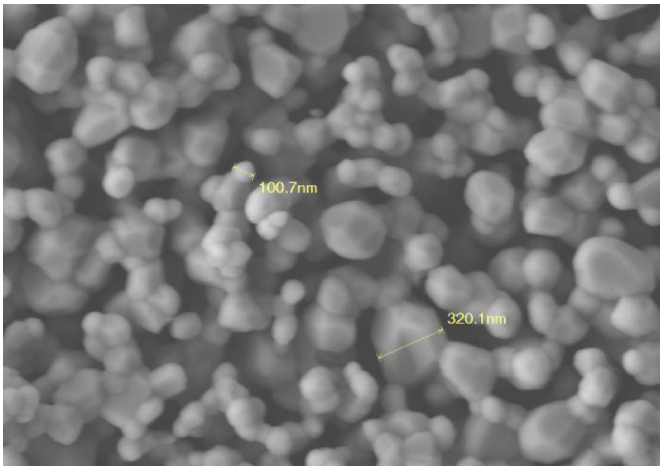

Fig. 4. TEM photograph obtained for Nd:KY3F synthesized nanopowder after thermal treatment at T=550 °C.

(280 °C); d=14 nm (400 °C); d=73 nm (500 °C) and d=198 nm (550 °C)

ii) Yd:Nd:Tm:KY3F
d=11 nm (as grown −25 °C); d=11 nm (T=280 °C); d=11 nm (400 °C); d=25 nm (475 °C); d=17 nm (500 °C); d=139 nm (550 °C) and d=156 nm (600 °C).

Optical absorption spectrum of KY3F doped Yb:Nd:Tm bulk crystal has two main absorptions in the near infrared around 960 nm (Yb^{3+}) and around 800 nm due to Nd^{3+} and Tm^{3+} ions [10]. The most intense absorption is near 960 nm due to high concentration of ytterbium in the samples (10%). The absorption of Tm^{3+} near 800 nm in Yb(10):Nd(1.3):Tm(0.5):KY3F synthesized nanocrystals (as grown) is observed to be centered at 802 nm as is observed for the bulk crystal and has some additional lines for the $^4I_{9/2} \rightarrow {}^4F_{5/2}$ transition (centered at 802 nm) compared to the absorption measured for the bulk crystal (not shown in this work). It is observed also that its absorption structure tends to fit the bulk absorption structure as the temperature of the thermal treatment increases to T=550 °C. This indicates that crystallinity of the nanoparticle enhanced for the heat treatment at T=550 °C.

When Yb:Nd:Tm:KY3F bulk crystal is excited at 802 nm, blue (470–480) nm Tm^{3+} - emission is observed and the blue emission strongly increases for neodymium concentration of 1 mol% [9]. This luminescence effect indicates that Nd^{3+} ions significantly contribute to the population of the $^1G_4$ excited level that emits around 480 nm. Fig. 5 shows the schematic energy diagram levels of Yb/Nd/Tm proposed for Tm^{3+} ($^1G_4$) upconversion, which will be discussed and proved to be essential for the blue emission of nanocrystals taking into account the luminescence dynamics analysis in the sequence. When the Yb:Nd:Tm samples are excited at (797–802) nm the following processes are observed to compete (Up_1 and Up_2):

1) (Nd × Tm) (Up_1):
Nd^{3+} ($^4F_{3/2}$)+Tm^{3+} ($^3H_4$)→Nd^{3+} ($^4I_{11/2}$)+Tm^{3+} ($^1G_4$)
2) (Nd × Yb × Tm) (Up_2)
Nd^{3+} ($^4F_{3/2}$)+Yb^{3+} ($^2F_{7/2}$)→Nd^{3+} ($^4I_{11/2}$)+Yb^{3+} ($^2F_{5/2}$),
Yb^{3+} ($^2F_{5/2}$)+Tm^{3+} ($^3H_4$)→Yb^{3+} ($^2F_{7/2}$)+Tm^{3+} ($^1G_4$)

The luminescence kinetic of an acceptor state that is indirectly excited by the donor–acceptor (or D–A) energy transfer is given by Eq. (1), which has been derived elsewhere [17] for an energy transfer that includes Burshtein (or Inokuti–Hirayama, where ω=0) model for the donor decay due to a dipole–dipole

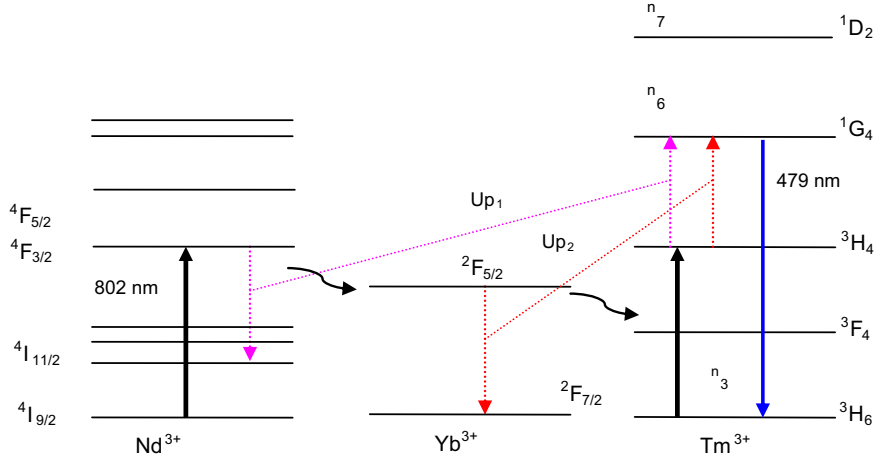

Fig. 5. Energy levels diagram of Yb:Nd:Tm:KY3F nanocrystal.

interaction [18].

$$I_1(t) = I_0\left\{\exp\left(-\frac{t}{\tau_A}\right) - \exp\left(-\frac{t}{\tau_d} - \omega t - \gamma\sqrt{t}\right)\right\}, \quad (1)$$

where τ_A is the luminescence lifetime of the acceptor (A) excited state and τ_d is the intrinsic lifetime of the donor (D) excited ion. γ is the energy transfer parameter (given in $s^{-1/2}$) due to the donor to acceptor direct transfer and ω is the energy transfer parameter (given in s^{-1}) due to the migration contribution through donor excited level. The first term of Eq. (1) gives the luminescence decay of the acceptor and the second gives the luminescence risetime, which should be equal to the donor total lifetime. The risetime constant was obtained by integration according to Eq. (2) for the case of a non-exponential process.

$$\tau = \int_0^\infty \exp\left(-\frac{t}{\tau_d} - \omega t - \gamma\sqrt{t}\right) dt. \quad (2)$$

For instance, if the diffusion process between donor states dominates the energy transfer mechanism (or $\omega \gg \gamma^2$) the donor decay will be exponential and the acceptor risetime will be exponential. That is the case observed of all the Nd→or Yb→Tm transfers in Yb:Nd:Tm systems observed in this work because of the high Yb^{3+} concentration used (>5 mol%). In this case, the acceptor luminescence fitting was performed using Eqs. (3) and (4) that has been used to describe the upconversion kinetic [10,19–22].

$$I_1(t) = A\exp(-t/t_1) + B\exp(-t/t_2) - (A+B)\exp(-t/t_3), \text{ where } t_3 < t_1, t_2 \quad (3)$$

$$I_2(t) = A\exp(-t/t_1) + B\exp(-t/t_3) - (A+B)\exp(-t/t_2), \text{where } t_2 < t_1,\ t_3. \quad (4)$$

The fitting parameters t_1 and t_2 are the characteristic time of the upconversion processes Up_1 and Up_2 and t_3 is the luminescence lifetime of the $^1G_4$ level of Tm^{3+}. Parameters A and B are the amplitude of the Up_1 and Up_2 upconversion processes, respectively for the case of $t_3 < t_1$, t_2.

The emission spectrum of $^1G_4 \rightarrow {}^3H_6$ (Tm^{3+}) transition is shown in Fig. 6 for the nanopowder and bulk crystal excited by pulsed laser at 802 nm (E=5.4 mJ, 4 ns). It is seen that the emission intensity of nanocrystals grows up as the thermal treatment temperature (TT) increases to 600 °C. Fig. 7 shows the intensity increasing of the 482 nm upconversion emission of Tm^{3+} as a function of the temperature of TT and that its intensity grows up strongly for TT > 500 °C.

The upconversion luminescence kinetic at 479 nm due to the $^1G_4$ level emission of Tm^{3+} is induced by the pulsed laser excitation at 802 nm for Yb:Nd:Tm:KY3F nanopowder and bulk crystal and the measurements are shown in Fig. 9. Best fit of 479 nm emission of nanopowder was performed using $I_2(t)$ expression given by Eq. (3) (for the case where $t_3 < t_1$, t_2) from where best fitting parameters t_3=1.8 μs, t_1=47 μs and t_2=366 μs are the derived parameters using a least squares fit with a correlation coefficient equals to 0.996. It is noticeable that the 479 nm emission transient measured for the nanocrystal (TT=25 °C) has two time constants t_1 and t_2 due to the (Nd × Tm) (Up_1) and (Nd × Yb × Tm) (Up_2) upconversion processes with contributions of 78% and 22%, respectively, and that these contributions change with the temperature of the thermal treatment, i.e., contributions are 33% for Up_1 and 67% (Up_2) for TT=550 °C. On the other hand, the 479 nm emission transient measured for the bulk crystal exhibits only one upconversion component (t_2) (see Fig. 8). Table 1 shows the characteristic time t_1 and t_2 for the upconversion processes (Up_1, Up_2) and the lifetime (t_3) of $^1G_4$ excited state of Tm^{3+} obtained from best fitting of the experimental luminescence kinetic using Eqs. (3) and (4) for Yb:Nd:Tm:KY3F synthesized nanopowder (25 °C) and after TT=300, 400, 475 and 550 °C.

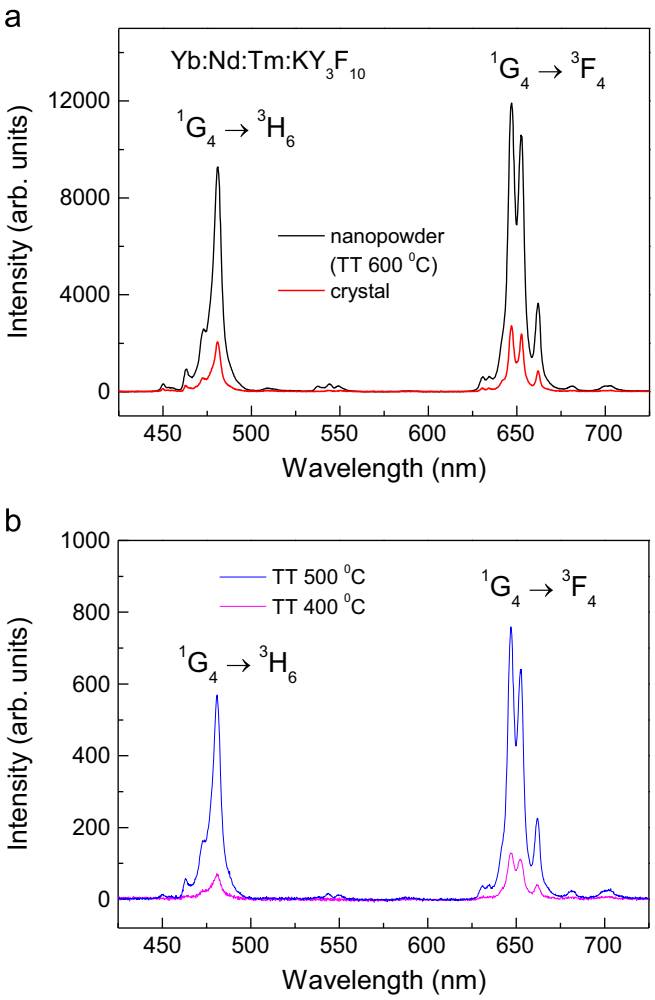

Fig. 6. Emission spectrum of Yb(10%):Nd(1.3%):Tm(0.5%):KY3F synthesized nanopowder after thermal treatments at 400, 500 and 600 °C and bulk crystal using pulsed laser excitation at 802 nm of 4 ns (10 Hz) with an average energy of 5.4 mJ. Solid red line was measured for the bulk crystal (Yb:Nd:Tm:KY3F) for comparison. (For interpretation of the references to color in this figure legend, the reader is referred to the web version of this article.)

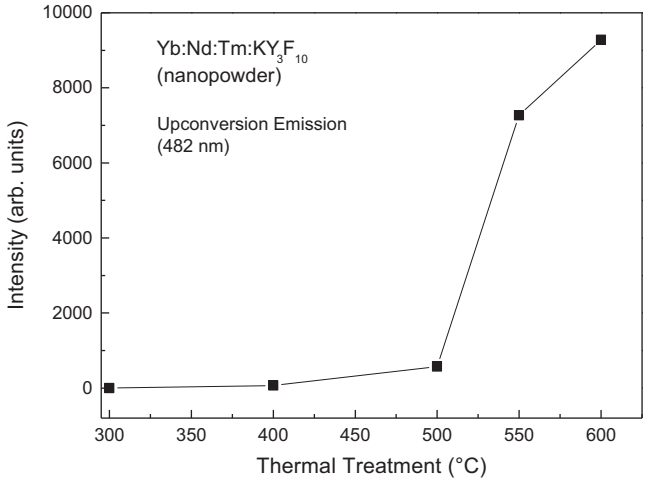

Fig. 7. Upconversion luminescence intensity measured at 482 nm after thermal treatments at T=300, 400, 500, 550 and 600 °C for Yb(10%):Nd(1.3%):Tm(0.5%):KY3F synthesized nanopowder using pulsed laser excitation at 802 nm.

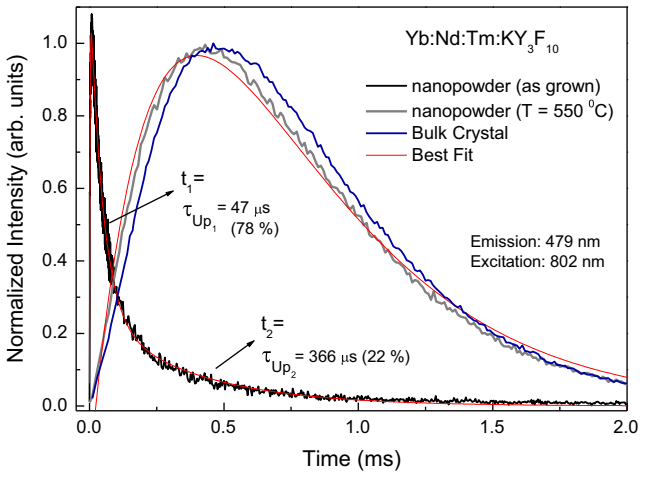

Fig. 8. Upconversion luminescence transient ($^1G_4$ level of Tm^{3+}) measured at 479 nm before (black line) and after TT=550 °C (gray line) for synthesized nanopowder and bulk crystal (blue line) of Yb(10 mol%):Nd(1.3 mol%):Tm(0.5 mol %):KY3F. Pulsed laser excitations at 802 nm with E=13.8 mJ and average intensity of 6 MW/cm^2 per pulse were used. The emission intensities were normalized to one in order to visually compare the strong differences between systems (bulk crystal and nanoparticles). (For interpretation of the references to color in this figure legend, the reader is referred to the web version of this article.)

From the results presented in Table 1, one can conclude that Up_1 and Up_2 processes contributions to the 479 nm luminescence of the nanopowder changes with the increase of thermal treatment temperature and that the luminescence kinetic (nanopowder after TT=550 °C) tends to fit the luminescence kinetic measured for the bulk crystal, which has only one upconversion (Up_2) component ($t_2=t_{rise}=376$ μs) and $^1G_4$ decay equal to $t_3=472$ μs. Using the experimental data given in Table 1 it was constructed Fig. 10, where Fig. 10(a) shows that the $^1G_4$ level lifetime (t_3) increases from 1.8 μs (25 °C) to $t_3=456$ μs (TT=550 °C) induced by the thermal treatment of nanopowder. The luminescence efficiency of $^1G_4$ excited level of Tm^{3+} was calculated using the relation Ef=t_3 (nanopowder, T)/t_3 (bulk crystal), where $t_3=472$ μs was obtained for the bulk crystal. Fig. 10(c) shows that $^1G_4$ luminescence efficiency (Ef) strongly augments with the increasing temperature to 550 °C, i.e., the initial Ef=0.38% (25 °C) changed to Ef=96% after TT=550 °C. This effect on t_3 might indicate that the existence of (Nd × Tm) interaction (Up_1 process) also produces the (Tm × Nd) cross-relaxation [$Tm^{3+}(^1G_4)$: $Nd^{3+}(^4I_{15/2})$] × [$Tm^{3+}(^3H_4)$: $Nd^{3+}(^4F_{3/2})$] that decreases the $^1G_4$ lifetime and introduces a repopulation time of $^3H_4$ (Tm^{3+}) excited level. Consequently it must affect the time constant t_2 of Up_2 process (Nd × Yb × Tm) by increasing its mean value mainly for the initial of the thermal treatments (T=400 °C) where the (Nd × Tm) interaction contributes for more than 50%.

Fig. 10(b) shows that characteristic time (t_1) of Up_1 process (Nd × Tm interaction) becomes longer as the temperature of thermal treatment increases to T=550 °C, while its contribution in the overall upconversion luminescence decreases, i.e., the initial contribution of Up_1 equals to 78% (25 °C) changed to 33% after TT=550 °C.

Finally it is observed that the characteristic time (t_2) of Up_2 process (Nd × Yb × Tm interaction) suffer a linear increasing for thermal treatments up to T=400 °C and a linear decreasing for $T>400$ °C (see Fig. 10(d)).

4. Discussion

The fact that two upconversion component mechanism are competing to the produce the blue upconversion luminescence of Tm^{3+} observed for nanocrystals (as grown) and that Up_1 contribution decreases as the temperature of the thermal treatment increases indicates that a concentration effect is responsible for this experimental observation. In particular, the Nd^{3+} ions distribution in the synthesized nanocrystals must be not uniform and must exhibit a strong concentration gradient that increases towards the nanoparticle surface in order to explain the observed effects on the 479 nm upconversion luminescence (the two upconversion components). Thermal treated nanocrystals at 550 °C presented only one upconversion component and it is similar to the bulk crystal upconversion luminescence, wherein it is assumed a uniform distribution of the dopants.

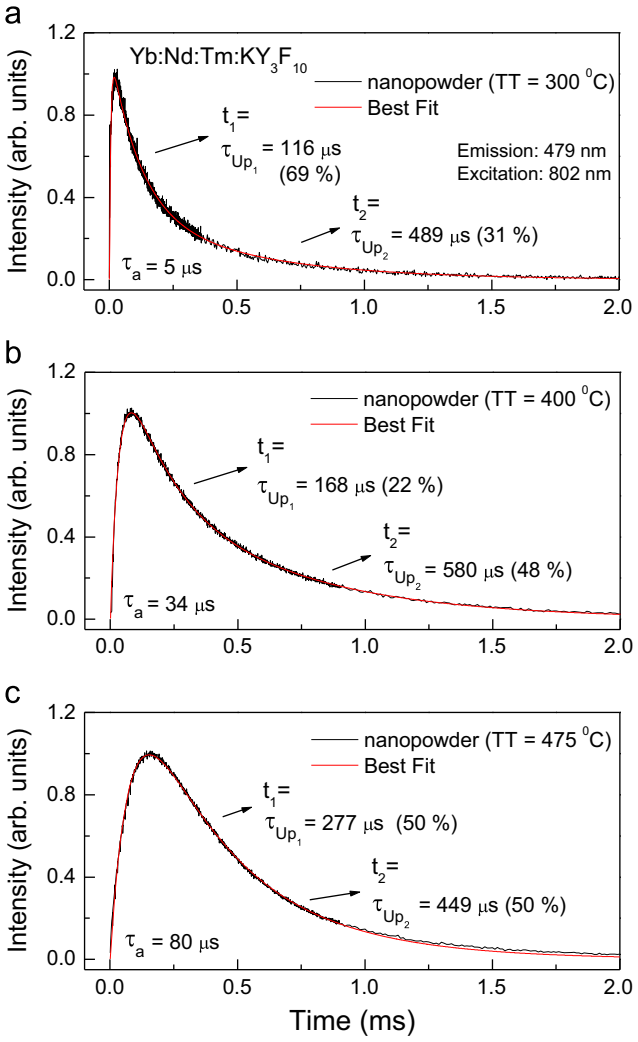

Fig. 9. Upconversion luminescence transient ($^1G_4$ level of Tm^{3+}) measured at 479 nm for nanopowder of Yb(10 mol%):Nd(1.3 mol%):Tm(0.5 mol%):KY3F after thermal treatments at T=300 (a), 400 (b) and 475 °C (c) using pulsed laser excitations at 802 nm (E=13 mJ). Best fit of luminescence transient was done using Eq. (3).

The observation of Up_1 process (78%) due to [$Nd^{3+}(^4F_{3/2})$ × $Tm^{3+}(^3H_4)$] cross-interaction in competition with Up_2 process (22%) due to $Nd^{3+}(^4F_{3/2})\rightarrow Yb^{3+}(^2F_{7/2})\rightarrow[Yb^{3+}(^2F_{5/2})\times Tm^{3+}(^3H_4)]$ for the synthesized nanocrystals corroborates with the assumption that the Nd^{3+} ions distribution is different than the observed for the bulk crystal.

Nanocrystals of KY3F single doped with 1.3 mol% of Nd^{3+} were also obtained to measure the luminescence lifetime of $^4F_{3/2}$ excited level of Nd^{3+} before (25 °C) and after several thermal treatments having $T<600$ °C. Fig. 11 shows the $^4F_{3/2}\rightarrow{}^4I_{9/2}$ and $^4F_{3/2}\rightarrow{}^4I_{11/2}$

Table 1
Experimental values of the lifetime of $^1G_4$ excited state (t_3) and the upconversion time constants (t_1 and t_2) obtained from best fitting of experimental luminescence kinetic curves using Eq. (3) obtained for Yb:Nd:Tm:KY3F after TT=300, 400, 475 and 550 °C.

Thermal treatment	A	B	t_1 (Nd × Tm)	t_2 (Nd × Yb × Tm)	t_3 ($^1G_4$)	R^2
Time constants of upconversion processes (experimental)						
25 °C	0.923	0.257	47 ± 0.2 μs (78%)	365 ± 3 μs (22%)	1.77 ± 0.02 μs	0.996
300 °C	0.830	0.381	116 ± 2 μs (69%)	489 ± 4 μs (31%)	5.34 ± 0.02 μs	0.998
400 °C	0.817	0.742	168 ± 4 μs (52%)	580 ± 8 μs (48%)	34.4 ± 0.3 μs	0.999
475 °C	1	0.999	277 ± 9 μs (50%)	449 ± 4 μs (50%)	79.6 ± 0.5 μs	0.999
550 °C	3.80	3.72	453 ± 20 μs (33%)	314 ± 15 μs (67%)	456 ± 18 μs	0.996
Bulk crystal	–	–	–	376 ± 4 μs (100%)	472 ± 12 μs	0.985

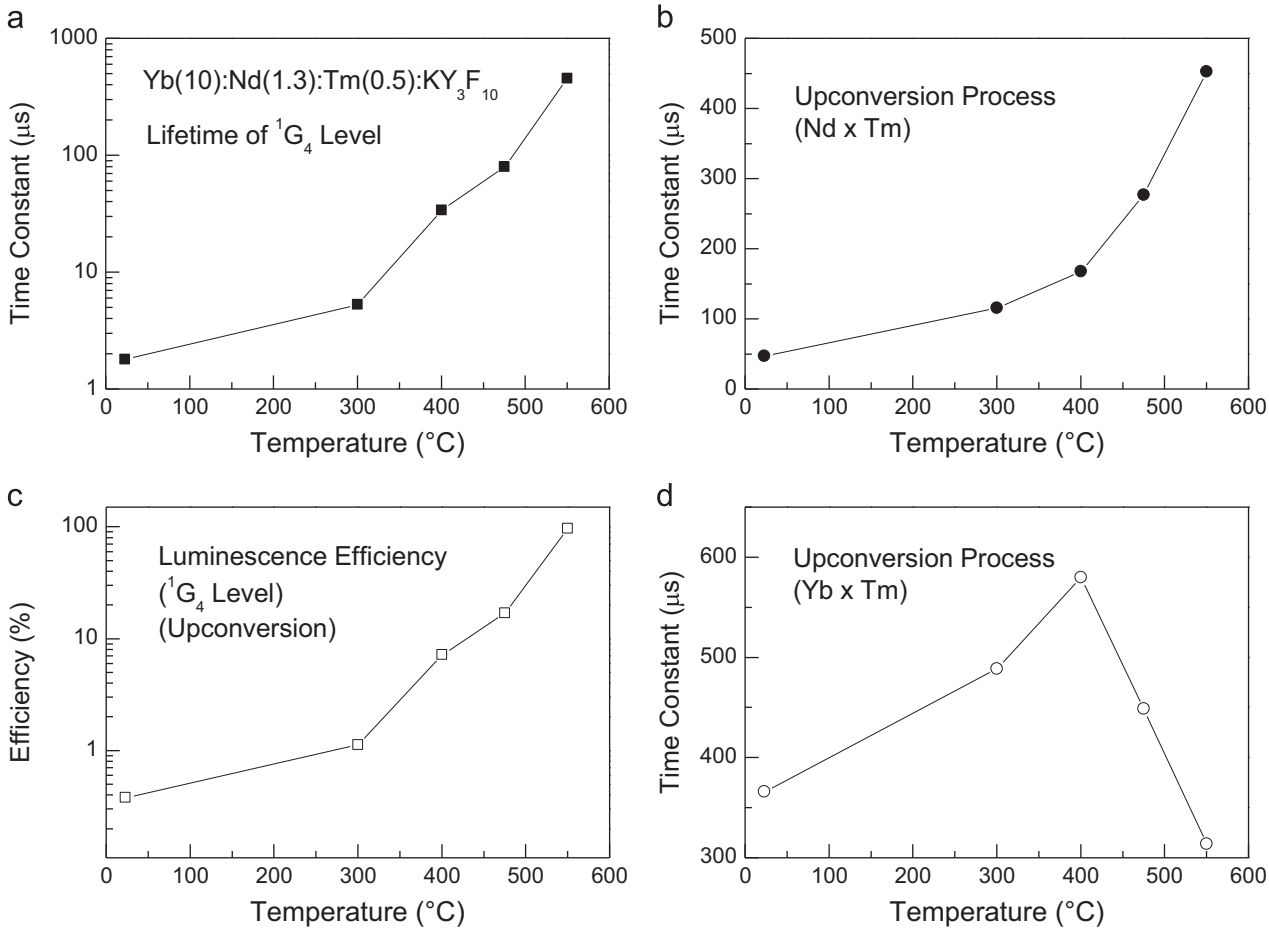

Fig. 10. Plot of measured lifetime of $^1G_4$ level of Tm^{3+} (a), luminescence efficiency ($^1G_4$) (c), and the upconversion time constants: (b) t_1 (Up_1) and (d) t_2 (Up_2) for Yb(10): Nd (1.3 mol%):Tm(0.5 mol%): KY3F synthesized nanopowder after many thermal treatments up to T=550 °C.

emission transitions of Nd^{3+} for the synthesized nanopowder (25 °C) and after several thermal treatments, where one can see that the emission intensity increases with increasing temperature of thermal treatments.

Fig. 12 shows the emission decay of $^4F_{3/2}$ level of Nd^{3+} measured at 886 nm for KY3F nanocrystals before and after thermal treatments with TT=150, 280, 400 and 550 °C. Best fitting of the emission decay was performed using Burshtein model [18] and the best fitting parameters are given in Table 2. The results presented in Table 2 shows that the emission decays are not exponential (γ parameter is large) and that the $^4F_{3/2}$ lifetime strongly depends on the thermal treatment temperature, i.e., the lifetime of 26 μs measured for the synthesized nanocrystal (25 °C) increases to τ=388 μs after TT=550 °C. The luminescence efficiency of $^4F_{3/2}$ excited level of Nd^{3+} for Nd:KY3F nanopowder after thermal treatment was calculated using the relation Ef=τ (T)/τ (T=550 °C), where τ=388 μs was obtained after thermal treatment at T=550 °C. Fig. 13(a) shows that the luminescence efficiency of $^4F_{3/2}$ (Nd^{3+}) emission strongly increases with the thermal treatment temperature enhancement. Nevertheless, it is observed that the average size (from Rietveld method) of nanoparticles remains constant (12–14 nm) for thermal treatments with T < 430 °C, and growing only for higher thermal treatment temperatures (T > 430 °C). This result clearly shows that the mechanism responsible for the increasing of the luminescence efficiency of $^4F_{3/2}$ level (Nd^{3+}) is not dependent on the crystal size. However, this result indicates that the luminescence efficiency of $^4F_{3/2}$ level enhances at expenses of the (Nd × Nd) cross-relaxation decreasing for nanocrystals thermal treated with $T \geq$ 100 °C.

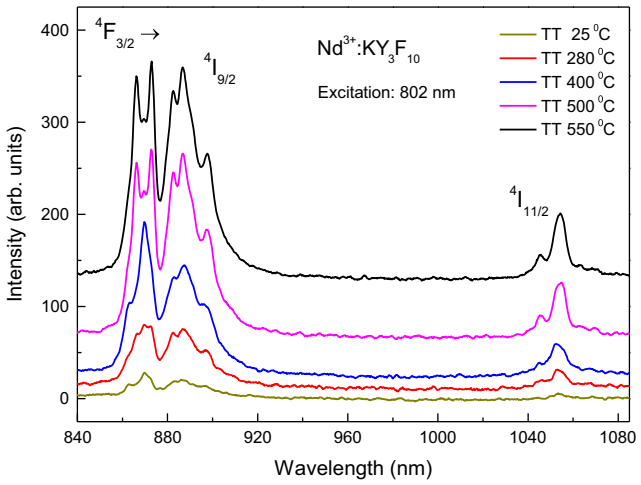

Fig. 11. Emission spectrum of Nd^{3+} (1.3 mol%) in KY3F measured for synthesized nanopowder (as grown) (25 °C) and after thermal treatments (TT=280, 400, 500 and 550 °C). A pulsed laser excitation at 802 nm of 4 ns of time duration (10 Hz) with a mean energy of 8 mJ was used.

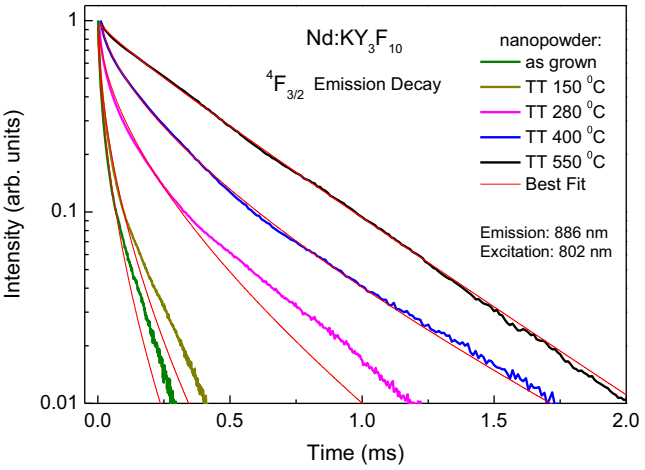

Fig. 12. Emission decay of $^4F_{3/2}$ excited level of Nd^{3+} in KY3F (1.3 mo l%) measured at 886 nm for the synthesized nanopowder (25 °C) and after several thermal treatments at T=150, 280, 400 and 550 °C. A pulsed laser excitation at 802 nm of 4 ns (10 Hz) with a mean energy of 10 mJ was used.

Table 2
Best fitting parameters of $^4F_{3/2}$ (Nd^{3+}) emission decay (886 nm) for the nanopowder (Nd:KY3F) as grown (25 °C) and after several thermal treatments with TT=150, 280, 400 and 550 °C. t_d is the exponential component of decay (includes excitation migration) and γ ($s^{-1/2}$) is the transfer parameter that does not includes migration. τ is the luminescence lifetime calculated using Eq. (2).

Thermal treatment	γ ($s^{-1/2}$)	t_d	R^2	τ (integrated)
Best fitting parameters of $^4F_{3/2}$ (Nd^{3+}) decay (experimental)				
25 °C	298 ± 1.3	1.0 ± 0.02 ms	0.999	26 μs
150 °C	238 ± 1.6	1.0 ± 0.02 ms	0.995	39 μs
280 °C	117 ± 1.3	1.0 ± 0.03 ms	0.991	121 μs
400 °C	83 ± 0.5	1.2 ± 0.02 ms	0.999	224 μs
550 °C	14 ± 0.2	0.51 ± 0.01 ms	0.999	388 μs

The $[Nd^{3+}(^4F_{3/2}) \times Nd^{3+}(^4I_{9/2})]$ cross-relaxation rate (W_{CR}) can be calculated using the equation $1/\tau = 1/\tau_i + W_{CR}$, where τ is the luminescence lifetime (experimentally measured) given in Table 2. τ_i is the intrinsic lifetime of $^4F_{3/2}$ level equal to 550 μs (measured for bulk crystal). Fig. 14 shows the values of W_{CR} (s^{-1}) calculated for many temperatures of thermal treatments for Nd:KY3F nanopowder. One can use the Arrhenius model (first order process) to

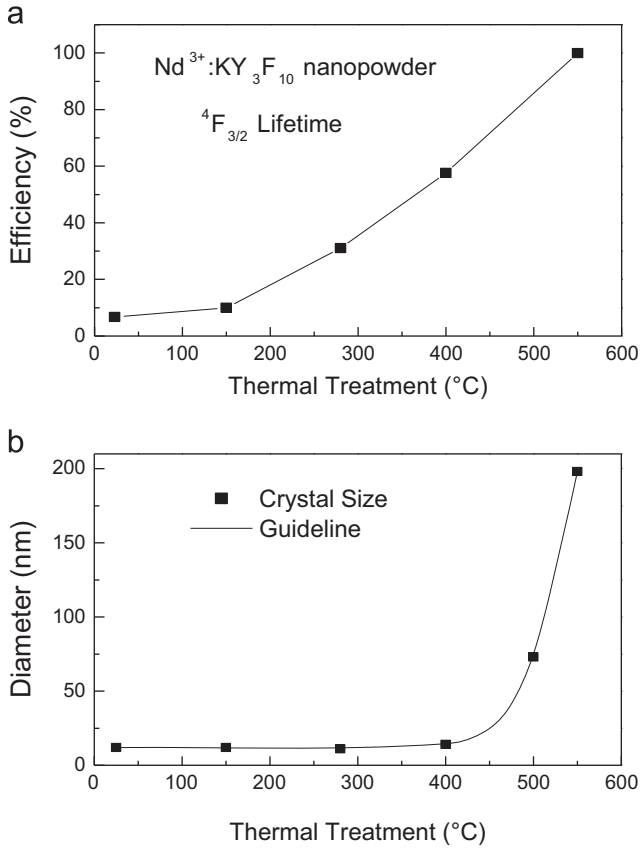

Fig. 13. Luminescence efficiency of $^4F_{3/2}$ level of Nd^{3+} ion (a) and the mean diameter (or crystal size) (b) measured as a function of thermal treatment temperature of Nd(1.3 mol%):KY3F synthesized nanopowder.

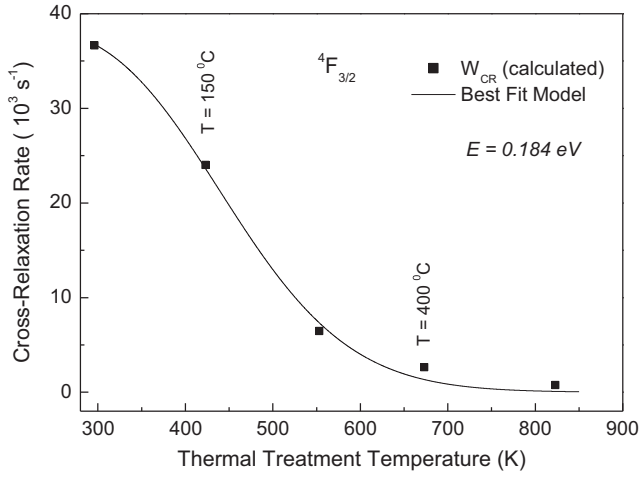

Fig. 14. Calculated cross-relaxation rate (s^{-1}) for (Nd × Nd) interaction plotted as a function of the thermal treatment temperature (K) for the Nd(1.3 mol%):KY3F nanopowder. Best fitting to the experimental data was done using Eq. (7).

describe the cross-relaxation dependence on temperature exhibited in Fig. 14 as follows:

1) The initial Nd^{3+} concentration (or ion distribution) produced in the synthesized nanocrystal (T=25 °C) will depend exponential on time duration (t) and temperature (T) of the thermal treatment as:

$$N(t) = N_0 \exp(-\alpha t); \quad \alpha = 1/\tau_{relax}; \quad \tau_{relax} = \tau_0 \exp(E/KT), \qquad (5)$$

where N_0 is the initial concentration (Nd), τ_{relax} is the relaxation time or the average time for the ion jump, E is the energy barrier (or activation energy) needed for the ion jump over the barrier, K is the Boltzmann constant, T is the temperature (Kelvin), and t is the time duration of thermal treatment at temperature T. Eq. (5) can be written also as

$$N(t,T) = N_0 \exp[-(t/\tau_0)\exp(-E/KT)] \quad (6)$$

2) assuming that W_{CR} is dependent on the square of [Nd] concentration one can have the following function describing the [Nd^{3+} ($^4F_{3/2}$) × Nd^{3+} ($^4I_{9/2}$)] cross-relaxation rate as a function of the thermal treatment temperature (T) considering a time duration constant (or $t=c$) for each treatment for nanocrystals

$$W_{CR}(T) = W_0 \exp(-a \times \exp(-b/T)), \quad (7)$$

where W_0, a and b are the fitting parameters.

Fig. 14 shows the best fit curve to fit W_{CR} versus thermal treatment temperature (T) by using Eq. (7) giving the fitting parameters $W_0 = 38828 \pm 1921\ s^{-1}$, $a = 85.6 \pm 49.1$ and $b = 2179 \pm 302$ K ($R^2 = 0.996$). Using that $b = E/K$, where $K = 8.333 \times 10^{-5}$ eV/K we obtained the activation energy equal to $E = 0.184$ eV. This experimental value of E (0.184 eV) for the Nd^{3+} ion diffusion assisted by yttrium vacancy migration is consistent with the activation energy found in experiment of ionic diffusions of Ag^{++} ions in α-Cu_2S crystals ($E = 0.198$ eV), Li^+ ions in α-AgI (0.198 eV), Au^+ ions in KCl (1 eV) and Pb^{++} ions in PbI_2 crystals (1.29 eV) [23].

Our proposed model states that the luminescence growth of $^4F_{3/2}$ (Nd^{3+}) and $^1G_4$ (Tm^{3+}) levels observed to increase with the increasing of the thermal treatment temperature, respectively for the Nd:KY3F and Yb:Nd:Tm:KY3F synthesized nanocrystals, is due to the gradual change of the initially Nd^{3+} ion distribution accomplished by the fast nanocrystals growth process. Nevertheless, the diffusion of Nd^{3+} ions assisted by yttrium vacancies migration from nanoparticle surface toward its interior, which propitiates the stress reduction of nanoparticles surfaces, also helps the system to get a more uniform distribution of Nd^{3+} ions for all volume of the nanoparticle. This mechanism explains the luminescence increasing in both crystals: i) the (Nd × Nd) cross-relaxation effect observed by the increasing of the luminescence efficiency of $^4F_{3/2}$ level of Nd^{3+} in Nd:KY3F under thermal treatment ($T > 100$ °C) and ii) the (Nd × Tm) cross-interaction leading to the increasing of the luminescence efficiency of $^1G_4$ level of Tm^{3+} in Yb:Nd:Tm:KY3F ($T > 100$ °C).

5. Conclusions

One conclusion of this work is that the non-adiabatic and fast growth of nanocrystals will introduce a non-random ions distribution that tends to increase the dopant concentration near the nanoparticle surface. The lifetime of $^4F_{3/2}$ state of Nd^{3+} is a good reference parameter to indirectly evaluate how is the Nd^{3+} ions distribution in the nanoparticle before and after thermal treatments because this level has a strong concentration effects due to the (Nd × Nd) cross-relaxation that reduces the luminescence efficiency. Second conclusion is that the concentration gradient found in the Yb:Nd:Tm:KY3F synthesized nanocrystals triggered the (Nd x Tm) interaction responding for the 78% of the blue upconversion, however decreasing the $^1G_4$ (Tm^{3+}) lifetime (2 μs) and consequently its luminescence efficiency to 0.38% due to the (Tm x Nd) reverse cross-interaction. Nevertheless, the thermal treatment at $T = 550$ °C can restore the luminescence efficiency of $^1G_4$ excited state to 98% when compared to the bulk crystal, however introducing a nanoparticle size augmentation (12→198 nm).

Acknowledgments

The authors thank financial support from FAPESP, Brazil (Grants nos. 1995/4166-0 and 2000/10986-0) and CNPq, Brazil.

References

[1] H. Zheng, D. Gao, X. Zhang, E. He, J. Appl. Phys. 104 (1) (2008) 013506.
[2] Z. Chen, H. Chen, H. HU, M. Yu, F. Li, Q. Zhang, Z. Zhou, T. Yi, C. Huang, J. Am. Chem. Soc. 130 (10) (2008) 3023.
[3] J. Zhou, F. Li, Chem. Soc. Rev. 41 (2012) 1323.
[4] N.P. Barnes, IEEE J. Sel. Top. Quantum Electron. 13 (2007) 435.
[5] K. Friese, H. Kruger, V. Kahlenberg, T. Balic-Zunic, H. Emerich, J-Y. Gesland, A. Grzechnik, J. Phys.-Condens. Matter 18 (2006) 2677.
[6] E. Boulma, M. Diaf, J.P. Jouart, M. Bouffard, J.L. Doualan, R. Moncorge, Opt. Mater. 30 (7) (2008) 1028.
[7] M. Ito, S. Hraiech, C. Goutaudier, K. Lebbou, G. Boulon., J. Cryst. Growth 310 (2008) 140.
[8] K.J. Kim, A. Jouini, A. Yoshikawa, R. Simura, G. Boulon, T. Fukuda, J. Cryst. Growth 299 (2007) 171.
[9] I.M. Ranieri, L.C. Courrol, A.F. Carvalho, L. Gomes, S.L. Baldochi, J. Mater. Sci. 42 (2007) 2309.
[10] H.M.S.M.D. Linhares, A.F.H. Librantz, L. Gomes, L.C. Courrol, S.L. Baldochi, I. M. Ranieri, J. Appl. Phys. 109 (2011) 08353.
[11] J.W. Mullin, Crystallization, 4th ed., Butterworth-Heinemann, Oxford, Boston, 2001.
[12] H.E. Buckley, Crystal Growth, Chapman and Hall, London, 1952.
[13] C. Sassoye, G. Patriarche, M. Mortier, Opt. Mater. 31 (8) (2009) 1177.
[14] A.C. Larson, R.B. Von Dreele, General structure analysis system (GSAS), 2000 (Los Alamos national laboratory report LAUR 86-748).
[15] B.H. Toby, J. Appl. Cryst. 34 (2001) 210.
[16] Th. H. de Keijser, E.J. Mittemeijer, H.C.F. Rozendaal, J. Appl. Cryst. 16 (1983) 309.
[17] L.D. da Vila, L. Gomes, L.V.G. Tarelho, S.J.L. Ribeiro, Y. Messaddeq, J. Appl. Phys. 93 (2003) 3873.
[18] A.I. Burshtein, JETP Lett. **35** (1972) 885.
[19] A.F.H. Librantz, L. Gomes, J. Lumin. 129 (2009) 376.
[20] L. Gomes, M. Oermann, H. Ebendorff-Heidepriem, D. Ottaway, T. Monro, S. D. Jackson, J. Appl. Phys. 110 (2011) 083111.
[21] L. Gomes, S.D. Jackson, J. Opt. Soc. Am. B 30 (6) (2013) 1410.
[22] L. Gomes, J. Lousteau, D. Milanese, E. Mura, S.D. Jackson, J. Opt. Soc. Am. B 31 (3) (2014) 429.
[23] N.F. Mott, R.W. Gurney, Electronic Processes in Ionic Crystals, 2nd edition, Dover Publications, Inc., New York, 1964.